

# Effect of impurity layers on the electric transport properties of Ni thin films

C. Prados

*Instituto de Magnetismo Aplicado, RENFE-UCM-CSIC, P.O. Box 155, 28230 Las Rozas, Madrid, Spain  
and Department of Physics and Astronomy, University of Delaware, Newark, Delaware 19716*

D. V. Dimitrov and G. C. Hadjipanayis

*Department of Physics and Astronomy, University of Delaware, Newark, Delaware 19716*

(Received 15 September 1998; revised manuscript received 3 December 1998)

The evolution of the electrical properties of Ni thin films is reported as a function of the distance  $L$  between periodically inserted impurity layers of different elements. In all the cases the resistivity of the films increases with the decrease of  $L$ . The anisotropic magnetoresistance (AMR) is modified when  $L$  becomes comparable to the electron mean free path  $\lambda$ . The effect depends drastically on the magnetic nature of the impurity element. While an enhancement of the AMR with decreasing  $L$  is observed with  $3d$  impurity elements, the insertion of Ho  $4f$  impurity layers gives rise to a decrease of the AMR factor with decreasing  $L$ . The dependence of the magnetotransport properties with  $L$  has been analyzed and discussed within the Fuchs-Sondheimer approach. [S0163-1829(99)01414-9]

## I. INTRODUCTION

The study of the change of electrical transport properties with the magnetization state of a given material has attracted much attention in condensed-matter research. The driven forces for such an effort are manifold. They include not only the basic understanding but also the technological application of most of the galvanomagnetic effects and, particularly, the so-called magnetoresistance (MR). This effect refers to the change of electrical resistance under an applied magnetic field. In general, all the materials exhibit this property which ranges within several orders of magnitude, depending on the magnetic nature of material. In the traditional  $3d$ -based magnetic elements and their alloys,<sup>1</sup> MR is anisotropic with respect to the field direction; it increases when the field is parallel to the current (positive longitudinal MR) and decreases when the field is perpendicular to the current (negative transversal MR). Therefore this magnetoresistance is labeled as anisotropic (AMR), and its physical origin is attributed to the dependence of the electronic scattering on the magnetization orientation via spin-orbit coupling.<sup>1</sup> The study of heterogeneous magnetic systems, such as multilayered structures,<sup>2</sup> granular systems,<sup>3</sup> etc., has brought the discovery of a galvanomagnetic phenomenon called giant magnetoresistance (GMR). Here, the change of electrical properties with magnetization is related to spin-dependent scattering mechanisms. More recently, a type of magnetoresistive phenomenon has been reported in perovskite oxides<sup>4</sup> which, due to the huge values achieved, is called colossal magnetoresistance (CMR). It is related to insulator-metal transitions induced by antiferromagnetic-ferromagnetic transitions.

In spite of the high values of MR achieved in GMR and CMR systems,  $3d$  magnetic materials exhibiting AMR are still widely used in practical devices, as magnetic sensors and reading heads for recording systems. The main reasons are their softer magnetic properties and better response at room temperature. Beside the extensive literature reporting

the magnetoresistive properties of such a materials (see, for instance, Ref. 1), very recently, different studies on enhanced<sup>5</sup> and oscillating behavior<sup>6</sup> of AMR have been reported in ferro/ferromagnetic multilayered structures. In previous works, an enhancement effect of interface impurity layers on the AMR of a thin film has been detected<sup>7</sup> and analyzed<sup>8</sup> within the frame of the Fuch-Sondheimer approximation.<sup>9</sup> Experiments on Ni thin films with Co impurity layers were performed and the results fitted to the established formalism. In this paper, we have extended that study to Ni films with other different  $3d$  and  $4f$  ferromagnetic layer impurities. Overall electrical and magnetoresistive behavior is correlated with the particular properties of the inserted impurities.

## II. EXPERIMENT

Ni thin films with inserted impurity layers consist of Ni films with constant thickness (nominally 1500 Å) in which impurity layers were periodically intercalated. Samples were fabricated by dc magnetron sputtering on water-cooled Si (100) substrates. Deposition details are similar to those in Ref. 8. Impurity layers are deposits of a different element for which deposition time was chosen to grow a layer of 1 Å in thickness. This time is insufficient to fill a complete one-atom-thick layer, hence resulting in an impurity layer. The distance between consecutive impurity layers is denoted by  $L$ , and their number is varied in order to keep the total thickness of the films constant. Two series of Ni samples with impurity layers have been fabricated, using Fe and Ho as  $3d$  and  $4f$  ferromagnetic impurity elements, respectively, with  $L$  ranging between 10 and 300 Å. Results on these series are compared with those previously reported on Ni with Co ( $3d$ -ferro), Cu (nonmagnetic), and single Ni layers.

Samples were structurally characterized by low- and high-angle x-ray diffraction (XRD). Perpendicular grain size has been estimated from the full width at half maximum in the (111) Ni peak, using Scherrer's formula. Hysteresis loops

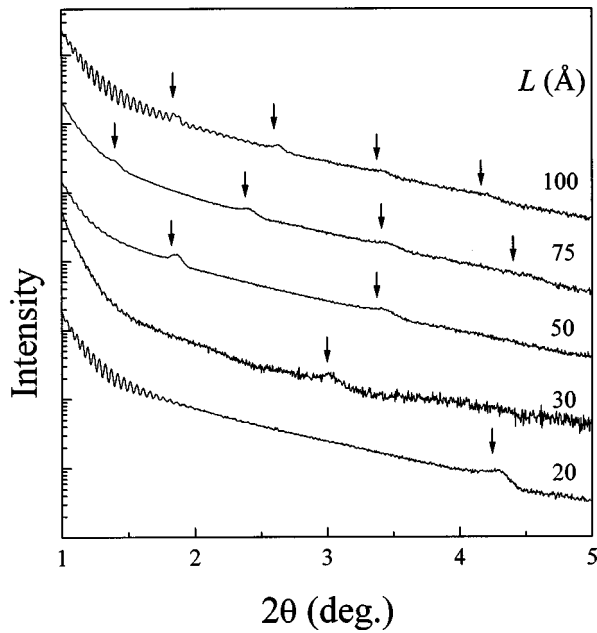


FIG. 1. Low-angle x-ray-diffraction pattern corresponding to the series  $[\text{Ni}_L/\text{Co}_1]_N$ .  $L$  stands for the distance between the 1-Å-thick impurity layers.  $N$  is the number of periods which varied in order to keep the total film thickness in 1500 Å. The arrows indicate the superlattice peaks corresponding to the impurity layers periodicity.

were measured at room and low temperatures by using a superconducting quantum interference device. In-plane and perpendicular configurations (determined by the magnetic-field direction with respect to the film plane) have been used. Resistivity and MR measurements were performed at different temperatures using the four-probe technique with in-line pressure contacts. The magnetic field was applied always along directions parallel to the film plane. Results shown in this work are on longitudinal magnetoresistance, where the voltage drop is measured along the direction of the electric current which is parallel to the applied field.

### III. RESULTS AND DISCUSSION

Low-angle XRD patterns indicate clearly that the impurity elements effectively form layers separated by a distance  $L$ . Figure 1 shows the low-angle patterns of Ni films with Co impurity layers periodically inserted at different distances  $L$ . Arrows mark the peaks corresponding to this superlattice periodicity. High-angle XRD spectra show that Ni is growing in the fcc structure with a preferred (111) direction along the direction perpendicular to the film plane for all the samples with different impurity elements and independently on the distance between the impurity layers. Figure 2 shows the grain size along the perpendicular-to-the-film direction as a function of  $L$  for samples with different impurity layers, Co, Fe, Ho, and Cu. Grain size increases very slightly with  $L$ , being in all the cases around 130 Å.

Magnetic measurements show the existence of a perpendicular magnetic easy axis, again independently of the impurity element and the parameter  $L$ . Also the coercive field does not depend substantially on the nature of the impurity element or the value of  $L$ . Typical values of coercivity and anisotropy field are 200 and 4000 Oe, respectively, at room

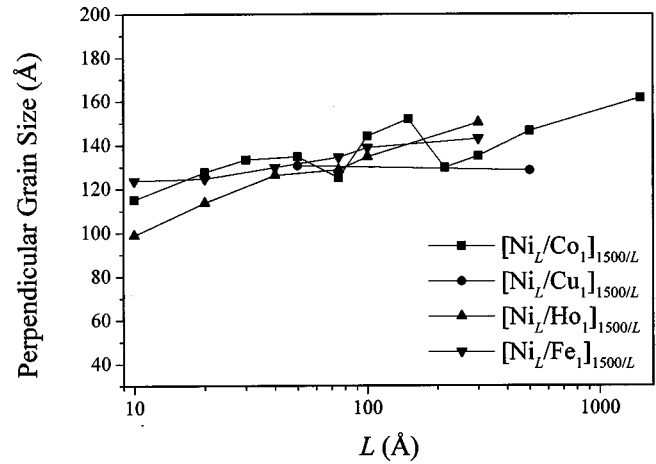


FIG. 2. Dependence of the perpendicular grain size on the distance between impurity layers,  $L$ , in films with different impurity elements (Co, Cu, Fe, and Ho).

temperature and 300 and 5000 Oe at 20 K. The out-of-plane magnetic anisotropy is attributed to the existence of a columnar growth structure which was observed by cross-sectional transmission electronic microscopy (TEM) in previous Ni films with Co impurity layers.<sup>8</sup> Those similar structural and magnetic properties indicate that the particular electric and magnetoresistive properties described below are directly related with the nature of the impurity element and not with differences in the structural and magnetic features of the samples.

Figure 3 shows the change of resistivity with temperature for samples with Fe and Ho impurity layers, and different

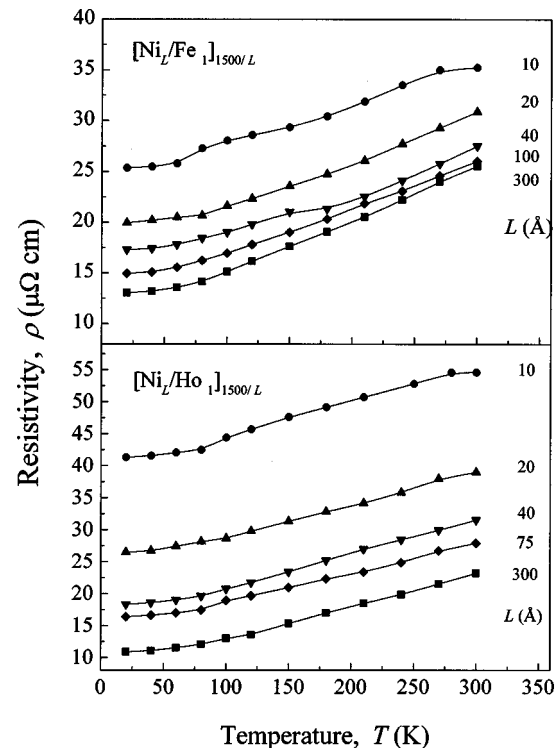


FIG. 3. Evolution of the electric resistivity with temperature in Ni films with Fe and Ho impurity layers and for different values of the distance between impurity layers.

values of  $L$ . The resistivity increases with the temperature and, also as in the case of the previously reported samples with Co and Cu impurities,<sup>8</sup> there is a systematic increase of resistivity with decreasing  $L$ . Although a similar trend is observed in the evolution of the resistivity with temperature and  $L$  for all the samples, films with Ho impurity layers behave differently from a quantitative point of view. Values of resistivity in Ho samples are typically twice the values in corresponding films with Co, Cu, or Fe impurity layers.

Magnetoresistance has been measured as a function of  $L$  for different temperatures and impurity elements. As in the previous cases, all the samples exhibit positive longitudinal AMR. The MR factor has been defined as  $\Delta R/R_c$ , where  $\Delta R$  is  $(R_s - R_c)$ , with  $R_s$  and  $R_c$  the resistance values at saturation and coercivity, respectively. Saturation data have been measured at the maximum available applied field (5.5 T).

Figure 4 shows the evolution of the MR factor with  $L$ , for samples with Fe, Co, Cu, and Ho impurity layers at three different temperatures. For large values of  $L$ , all the samples exhibit comparable MR factors at a given temperature, independently of the nature of the impurity element, and the values are similar to those measured in the pure Ni film (labeled with  $L = 1500 \text{ \AA}$ ). The effect of the impurity layers start to appear when  $L$  becomes comparable to the electron mean free path (mfp), as we discuss below. In the case of Fe impurities, the MR factor is increasing monotonously with decreasing  $L$ , having a maximum value around 2.7% at 20 K for  $L = 10 \text{ \AA}$ . Similar behavior was observed in samples with Co impurity layers, another  $3d$  ferromagnetic element. When the impurity is a nonmagnetic element, such as in the case of Cu, the MR factor is weakly sensitive to the change in  $L$ . However, a quite different trend is observed in samples with Ho  $4f$  impurity layers. The values of the MR factor are similar to those exhibited by films with Co, Fe, and Cu in the range of large values of  $L$ . However, when  $L$  becomes lower than the electron mfp, the MR factors are much lower and, contrary to the previous cases, they are decreasing with decreasing  $L$ . Figure 5 shows the evolution of  $\Delta\rho$  with  $L$  for samples with Fe and Ho as impurity elements ( $\Delta\rho = \rho_s - \rho_c$ , where  $\rho_s$  and  $\rho_c$  stand for the resistivity at saturation and coercivity, respectively). Notice that the MR factor can also be defined as  $\Delta\rho/\rho_c$ . We can observe that while  $\Delta\rho$  increases with decreasing  $L$  in Fe samples, the opposite trend is observed in samples with Ho as impurity element. This is clearly indicating that the anomalous decrease of MR with decreasing  $L$  in samples with Ho, is not an artificial effect due to the highest values of resistivity (shown in Fig. 3) and the definition of MR factor used. The MR factor is not decreasing with decreasing  $L$  only because of the large increase of the overall resistivity, but mainly because of the effective decrease in  $\Delta\rho$ .

Results are analyzed and discussed within the framework of a Fuch-Sondheimer approach,<sup>9</sup> previously developed in Ref. 8. Electrical resistivity in a film with periodically inserted impurity layers is obtained from the linearized Boltzmann equation in the relaxation time approximation. The effect of the impurity layers is considered by introducing a parameter  $\alpha$ , which accounts for the fraction of electrons diffusely scattered when they cross a given impurity layer. Solving the corresponding differential equation with these

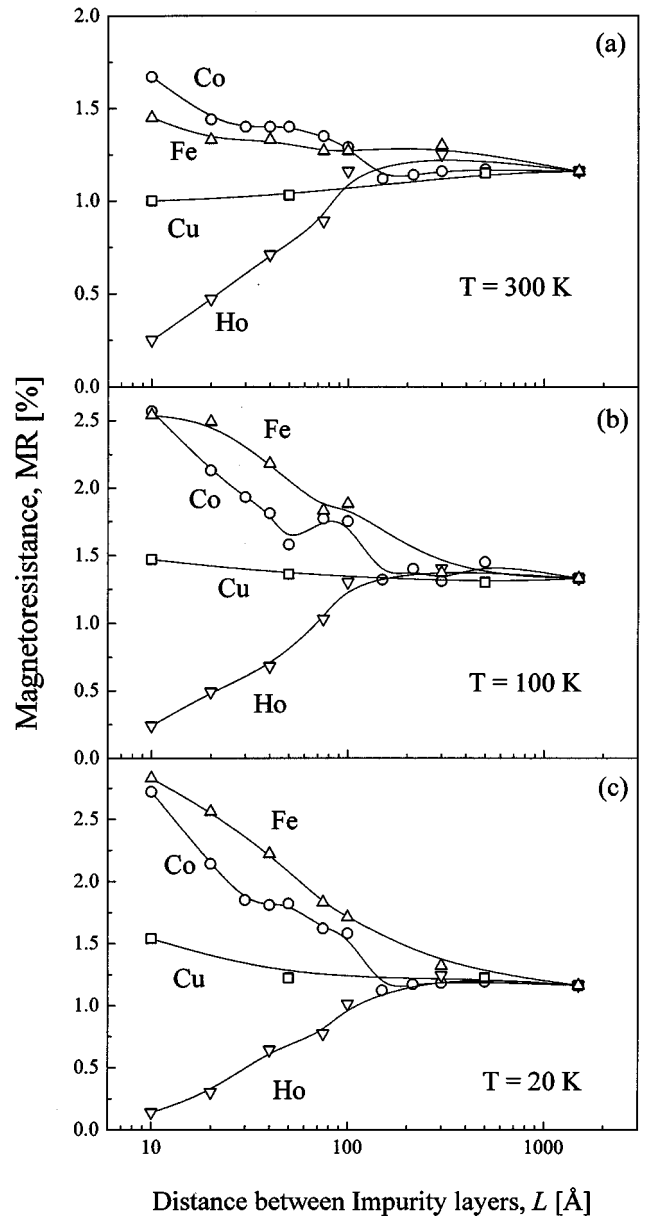


FIG. 4. Longitudinal MR as a function of the distance between impurity layers at three different temperatures and for four different impurity elements (Co, Cu, Fe, and Ho). Notice the different evolution of the MR factor depending on the magnetic nature of the impurity element. Lines are guides to the eyes.

boundary conditions, the resistivity  $\rho$  of the layer with inserted impurity layer is expressed as

$$\rho = \rho_0 \left( 1 + \frac{3}{8} \frac{\alpha \lambda}{L} \right), \quad (1)$$

where  $\lambda$  is the electron mfp and  $\rho_0$  represents the resistivity of a homogeneous Ni layer with the same thickness. This result indicates that the total resistivity of a film with impurity layers is composed of two contributions. First, a constant term  $\rho_0$  which accounts for the contribution to the total resistivity due to the bulk Ni. This term is equivalent to the resistivity of a pure Ni film with the same total thickness and similar microscopic structure than the sample with impurity layers. The second term represents the contribution of the

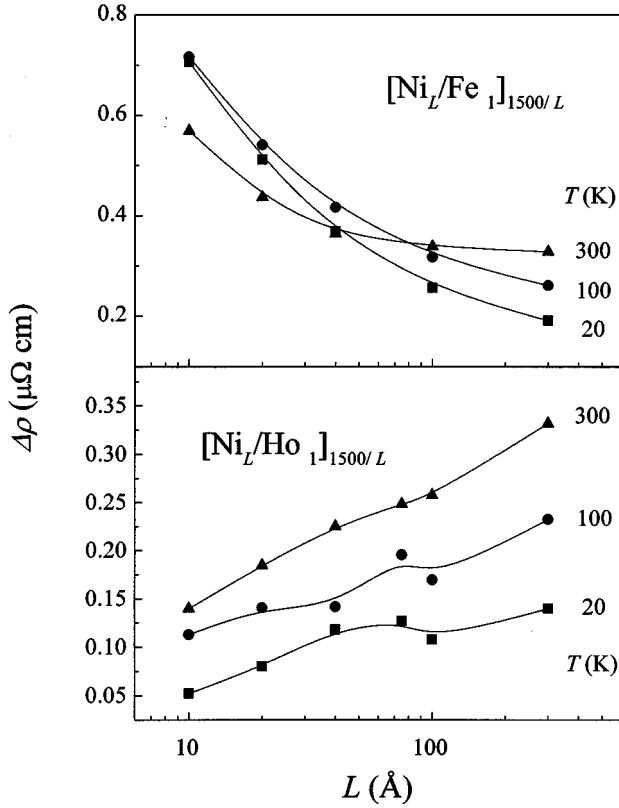


FIG. 5. Evolution of the change of resistivity with the magnetic state (coercivity and saturation) as a function of the distance between impurity layers at three different temperatures. Impurity elements are Fe and Ho, respectively.

electronic scattering at the inserted impurity layers to the total resistivity. It will perceptibly affect the total resistivity and MR factor when  $L$  becomes comparable to  $\lambda$ , as observed in the above reported experimental results. The dependence of resistivity on  $1/L$  accounts for the increase in resistivity with decreasing  $L$  as observed in Fig. 3.

The evolution of resistivity with  $L$  has been fitted to Eq. (1) at coercivity and magnetic saturation states. From this fitting process, values of  $\rho_0$  and  $\alpha$  have been obtained for both states. Two parameters have been defined in order to quantify the change of  $\rho_0$  and  $\alpha$  with the magnetization state. The change in  $\rho_0$  determines the Ni MR factor, which is the contribution to the total MR factor of the pure Ni in the films with inserted impurity layers. The change in the impurity layer scattering with the magnetization state is quantified through the definition of the *interface MR factor* (IMR) as  $(\alpha_s - \alpha_c)/\alpha_c$ , where the subindex corresponds to the saturation and coercivity state, respectively. Results from the fittings are summarized in Table I for films with Fe impurities. The values of the impurity scattering parameters  $\alpha$  and IMR are quite similar to those obtained for similar samples with Co as the impurity element.<sup>8</sup> As in that case, the Ni MR factor (MR attributed to bulk Ni) is much lower than the MR of the samples with low values of  $L$ , pointing out the effectiveness of the inserted impurity layers in the enhancement of MR when  $\lambda$  is comparable to  $L$ . Quite different results are obtained for films with Ho impurity layers, as summarized in Table II. The values of the electronic mfp at different tem-

TABLE I. Impurity layers scattering parameters, Ni MR and interface MR factor in Ni films with Fe impurity layers at different temperatures.

| $T$ (K) | $\alpha_{\text{coercivity}}$ | $\alpha_{\text{saturation}}$ | Ni MR (%) | IMR (%) |
|---------|------------------------------|------------------------------|-----------|---------|
| 300     | 0.3174                       | 0.3219                       | 1.25      | 1.28    |
| 100     | 0.3904                       | 0.4045                       | 1.8       | 3.6     |
| 20      | 0.3716                       | 0.3875                       | 1.5       | 4.28    |

peratures are similar to those in samples with Co and Fe and also the so-called Ni MR factor is very similar. This is indicating that the electric properties of the bulk are quite similar in all these samples within the studied range of temperatures and values of  $L$ . However, the impurity scattering parameters  $\alpha$  are larger for samples with Ho than those with Fe or Co by a factor of 3. This is attributed to the larger atomic size of Ho when compared to Ni, Fe, or Co, and hence, Ho impurity layers present a higher diffusely scattering effectiveness than the other elements (in fact, bulk electric resistivity is one order of magnitude larger in bulk Ho than in transition-metal elements). In Ho samples, the values of  $\alpha$  are close to one, indicating that almost every electron crossing a given Ho impurity layer is scattered. This result clarifies the origin of the larger values of resistivity observed in samples with Ho impurities with respect to those measured in films with the other impurity layers (Fig. 3). On the other hand, it is observed that the impurity scattering MR (IMR) of Ho is negative and lower in absolute value than in the case of Co and Fe. The negative value of IMR means that the scattering effect of the Ho impurity layers is, according to the definition of IMR, to decrease the resistivity when a magnetic field is applied, in contrast to the case of ferromagnetic  $3d$  elements. However, this result is not surprising, because the longitudinal MR of bulk Ho is negative,<sup>10</sup> that is, the longitudinal resistivity of bulk Ho decreases under an applied magnetic field (bulk Ho exhibits negative longitudinal MR), while in the case of ferromagnetic  $3d$  elements, the longitudinal magnetoresistance is positive.

All the previously presented results reinforce the idea that the scattering at the inserted impurity layers is related to a spin-orbit mechanism. The effect of inserting  $3d$  ferromagnetic elements enhances the AMR of Ni, while the effect with a nonmagnetic element as Cu is almost negligible. The particular electronic configuration of Ho, together with the sign of its spin-orbit coupling gives a negative longitudinal AMR factor in the bulk material. This behavior is translated to the case of Ni films with Ho impurity layers, giving rise to a decrease of MR with decreasing  $L$ , and negative values of IMR. The high anisotropy and magnetic moment of the  $4f$

TABLE II. Impurity layers scattering parameters, Ni MR and interface MR factor in Ni films with Ho impurity layers at different temperatures.

| $T$ (K) | $\alpha_{\text{coercivity}}$ | $\alpha_{\text{saturation}}$ | Ni MR (%) | IMR (%) |
|---------|------------------------------|------------------------------|-----------|---------|
| 300     | 0.9636                       | 0.9585                       | 1.27      | -0.56   |
| 100     | 0.9454                       | 0.9422                       | 1.5       | -0.34   |
| 20      | 0.918                        | 0.9152                       | 1.2       | -0.31   |

orbital in Ho could indicate that the absolute value of IMR in these samples should be larger than in  $3d$  impurity elements. The low values of IMR measured here for samples with Ho are attributed to the shield effect produced by the external electrons on the deep  $4f$  orbitals.

#### IV. CONCLUSIONS

The structural, electrical, and magnetic properties of Ni films of constant thickness with Fe and Ho periodically inserted impurity layers have been characterized, and compared to previously reported results on similar samples with Co and Cu as impurity elements. Control and reproducibility of the structural, magnetic, and bulk electric transport properties allowed us to analyze the effect of the different impurity layers on the total AMR by using the Fuchs-Sondheimer

approach. Fe insertion shows a similar effect with Co because of their similar magnetic behavior. The effect of Ho insertion is opposite to the effect of  $3d$  ferromagnetic elements but it is in good agreement with its bulk electrical properties.

The experimental results presented in this work support the effectiveness of the approach developed in Ref. 8 to discriminate and analyze the effect of the insertion of different impurity elements on the transport properties of thin films.

#### ACKNOWLEDGMENTS

This work was supported by NSF Grant No. DMR-9307676. C.P. thanks the Programa Científico de la OTAN for financial support.

- 
- <sup>1</sup>T. R. McGuire and R. Y. Potter, IEEE Trans. Magn. **11**, 1018 (1975).
- <sup>2</sup>M. N. Baibich, J. M. Broto, A. Fert, F. Nguyen Van Dau, F. Petroff, P. Ettiène, G. Creuzet, A. Friederich, and J. Chacelas, Phys. Rev. Lett. **61**, 2472 (1988).
- <sup>3</sup>J. Q. Xiao, J. S. Jiang, and C. L. Chien, Phys. Rev. Lett. **68**, 3749 (1992).
- <sup>4</sup>R. Von Helmolt, J. Wecker, B. Holzapfel, L. Schultz, and K. Samwer, Phys. Rev. Lett. **71**, 2331 (1993).
- <sup>5</sup>C. Prados, D. Garcia, F. Lesmes, J. J. Freijo, and A. Hernando, Appl. Phys. Lett. **67**, 718 (1995); J. M. Gallego, D. Lederman, T. J. Moran, and Y. K. Schuller, **64**, 2590 (1994).
- <sup>6</sup>J. M. Gallego, D. Lederman, T. J. Moran, and Y. K. Schuller, Phys. Rev. Lett. **74**, 4515 (1995).
- <sup>7</sup>F. Lesmes, A. Salcedo, J. J. Freijo, D. García, A. Hernando, and C. Prados, Appl. Phys. Lett. **69**, 718 (1996).
- <sup>8</sup>C. Prados, D. V. Dimitrov, C. Y. Ni, A. Hernando, and G. C. Hadjipanayis, Phys. Rev. B **56**, 14 076 (1997).
- <sup>9</sup>K. Fuchs, Proc. Cambridge Philos. Soc. **34**, 100 (1938); E. H. Sondheimer, Philos. Mag. Suppl. **1**, 1 (1952).
- <sup>10</sup>S. Legvold, in *Magnetic Properties of Rare Earth Metals*, edited by R. J. Elliot (Plenum, New York, 1972).